Available online at www.sciencedirect.com

ScienceDirect

Energy Procedia 77 (2015) 195 – 201

Energy Procedia

5th International Conference on Silicon Photovoltaics, SiliconPV 2015

Theoretical investigation of carrier-selective contacts featuring tunnel oxides by means of numerical device simulation

Heiko Steinkemper*, Frank Feldmann, Martin Bivour, Martin Hermle

Fraunhofer Institute for Solar Energy Systems ISE, Heidenhofstrasse 2, 79110 Freiburg, Germany

Abstract

Recently, a variety of different n-type Si solar cells with carrier-selective contacts featuring tunnel oxides achieving remarkable cell results has been presented. Theoretical investigations on this topic are rare, especially simulations actually accounting for tunneling through the oxide interlayer. In this work we investigate the influence of different parameters affecting the passivation quality and thus the device performance by means of numerical device simulation. Thereby, a fundamental understanding of solar cells with carrier-selective contacts featuring tunnel oxides is generated which is essential to further develop this promising technology.

Peer review by the scientific conference committee of SiliconPV 2015 under responsibility of PSE AG

Keywords: Device simulation; numerical simulation; tunneling; tunnel oxide, carrier-selective contacts

1. Introduction

In the last year, different n-type Si solar cells with carrier-selective contacts featuring tunnel oxides have been presented [1-3]. All concepts feature high open circuit voltages of up to 739 mV [2] due to the good passivation properties of the oxide layers and high conversion efficiencies of up to 24.4 % [4] have been reached. Experimentally different approaches for the passivated contact are presented. Especially the doped Si layer can be amorphous [2], polycrystalline [3] or partially crystalline [4]. Beside the remarkable technological results there have not been a lot of theoretical investigations on this topic. A recent theoretical investigation of solar cells featuring

* Corresponding author. Tel.: +49-761-4588-5097; fax: +49-761-4588-9250.
E-mail address: heiko.steinkemper@ise.fraunhofer.de

Peer review by the scientific conference committee of SiliconPV 2015 under responsibility of PSE AG
doi:10.1016/j.egypro.2015.07.027

oxide interlayers has been carried out under the assumption that the current transport is dominated by carrier transport through oxide pinholes rather than by tunneling through the oxide layer [5]. In this work, since tunneling is expected to be efficient for very thin oxides (< 20 Å) [6] and some of the cell concepts feature ultra-thin oxide layers (12-15 Å [2] and 14 Å [1]), we assume that current transport is a result of carrier tunneling through the ultra-thin oxide layer.

The investigation of the contact quality of tunnel oxide passivated electron contacts is carried out performing numerical device simulations using Sentaurus Device [7]. In this work we will focus on the simulation principles (including details on the optical simulation) and the basic results concerning the recombination properties by means of an analysis of the open circuit voltage.

2. Simulation setup

The here investigated device is based on the electron selective TOPCon approach of Ref. [4]. The optical simulation as well as the electrical simulation are performed with Sentaurus Device [7]. Using such a complex device simulation environment is essential for the detailed investigation of the rear side properties of the solar cell as presented in this work, featuring thin layer stacks, complex band structures and carrier tunneling.

2.1. Optical simulation

The optical simulation is performed using a 3D symmetry element representing a quarter (upright) pyramid of the front surface texture of the modeled solar cell. Front metal contacts are not actually modeled in the optical simulation. The optical shading is considered in the electrical simulation by scaling the optical generation in the device.

Sentaurus Device uses a combination of transfer matrix model for thin layers like the anti-reflection coatings (ARC) at the front and raytracing. The cell features a double ARC at the front on top of a thin Al_2O_3 passivation layer. The corresponding layer thicknesses are listed in Table 1. The complex refractive indices of the MgF_2 at the front and the Si layer at the rear are based on experimental data measured at the Fraunhofer ISE, the materials of the remaining thin layers are taken from the material database of Sentaurus Device.

Table 1. Materials and corresponding thicknesses of the thin layer stacks (front and rear) used in the optical simulation.

Layer	Material	Thickness
Front ARC 1	MgF_2	100 nm
Front ARC 2	SiN	50 nm
Front passivation	Al_2O_3	10 nm
Rear tunnel oxide	SiO_x	1.5 nm
Rear Si layer	a-Si(n)	20 nm

The rear of the device featuring a tunnel oxide was simulated using the tilted mirror approach [8, 9] which accounts for additional surface roughness of silicon solar cells coated with dielectrics when using the transfer matrix formalism.

The optical and the electrical simulation are coupled using a 1D photo generation profile. This 1D profile is created from the 3D optical simulation by integrating over layers of equal distance perpendicular to the surface of the front texture. This is done for each wavelength and then the depth dependent total optical generation (shown in Fig. 1) is calculated depending on the irradiation spectrum, in this case the standard AM1.5G solar spectrum. The front texture is not actually modeled in the electrical simulation and the 1D generation profile is applied to an approximated, planar device.

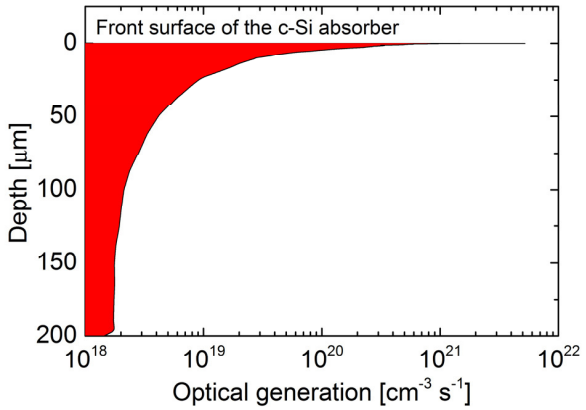

Fig. 1. 1D depth dependent optical generation calculated from the 3D optical simulation and using the AM1.5G solar spectrum. The depth of 0 µm corresponds to the front surface of the c-Si absorber.

Since the focus of this work is set on the electrical modeling of the device, the same generation profile is used for all electrical simulations. Minor deviations due to variation of the oxide thickness, the Si layer material and potential free carrier absorption in an additional diffusion at the rear do not significantly influence the results of the optical simulation and can therefore be neglected.

2.2. Electrical simulation

The full-area passivated rear contact of the device allows for a simple 2D symmetry element, which is depicted in Fig. 2. On the front it features a selective boron emitter design enabling high open circuit voltages of around 720 mV.

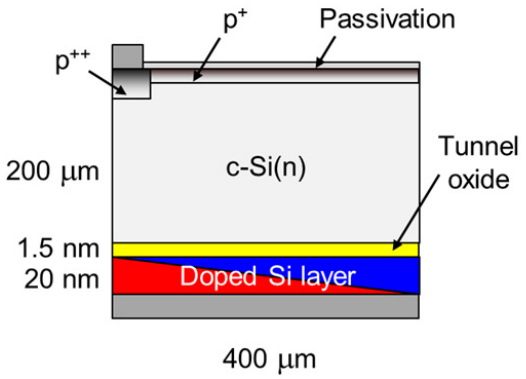

Fig. 2. 2D symmetry element for the electrical simulation carried out with Sentaurus Device.

On the rear the electron selective contact is created by an ultrathin tunnel oxide (1.5 nm) and an n-doped Si layer. The material parameters of the doped Si layer are one of the main objects of our investigation due to the different existing experimental approaches discussed in the introduction. A schematic band structure of the electron selective rear of the rear of the device is depicted in Fig. 3. The material parameters of the doped Si layer are varied by means of the electron affinity χ_0 and the band gap energy E_g. In this work we will discuss the two special cases for (i) amorphous silicon (χ_0 = 3.9 eV / Eg = 1.7 eV [10], red) and (ii) poly-crystalline silicon, represented by c-Si band parameters (blue). A more detailed variation of the band parameters and the doping of the Si layer will be published elsewhere.

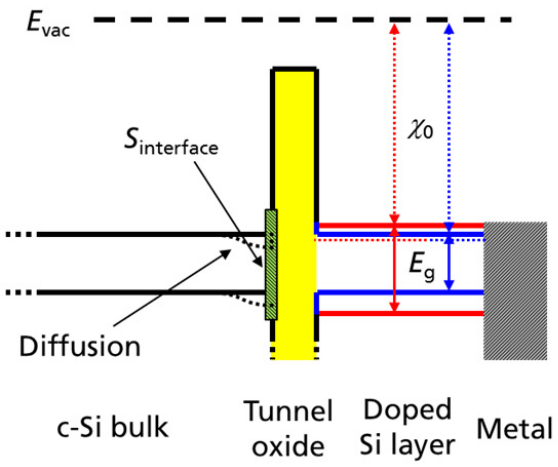

Fig. 3. Scheme of the band structure of the carrier selective contact featuring a thin tunnel oxide. Additionally the different parameters investigated in this study are depicted.

Further investigated parameters such as an additional in-diffusion in the c-Si bulk material (modeled by a Gaussian shaped n^{++}-profile) and the surface recombination velocity at the c-Si/oxide interface $S_{interface}$ are also indicated in Fig. 3. The simulations are also performed without an oxide interlayer. $S_{interface}$ is then the recombination velocity at the interface of the c-Si bulk material and the doped Si layer. The recombination velocity at the metal contact is set to thermal velocity.

The physical models used in this study are mainly based on the models proposed in the review on numerical simulation by Altermatt [11]. For Auger recombination the advanced model of Richter et al. [12] is implemented. This is done using a physical model interface (PMI). PMIs offer the possibility to provide new models via C++ functions, and Sentaurus Device loads the functions at run-time [7].

Carrier tunneling through the high band gap tunnel oxide is based on the model presented in Ref. [13]. The resulting tunneling current depends on several parameters depicted in Fig. 4.

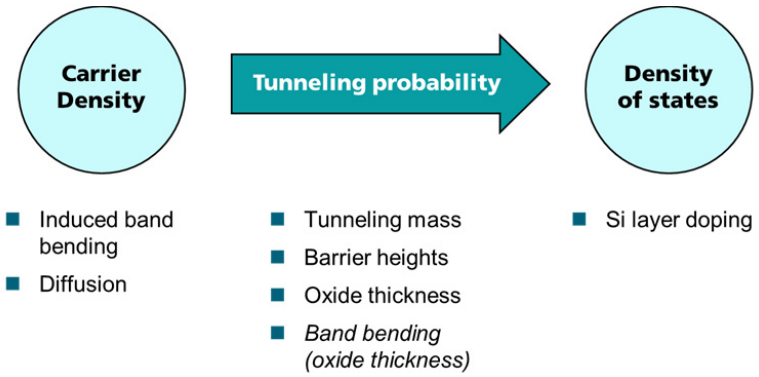

Fig. 4. Factors influencing the tunneling current through a potential barrier.

Basically, a carrier-selective contact is established when the minority carriers (here: the holes) are prevented from reaching the rear metal contact and therefore recombination of minority carriers at the metal surface is avoided. A possibility of achieving such a carrier selective contact is to choose the mentioned device parameters in such a manner that the tunnelling transport of holes through the tunnel oxide is prevented.

3. Results

In this chapter we investigate the recombination characteristics by means of the open circuit voltage V_{OC}. Fig. 5 shows the V_{OC} dependent on the surface recombination velocity $S_{interface}$ for different Si layer band parameters simulated with (left) and without tunnel oxide (right).

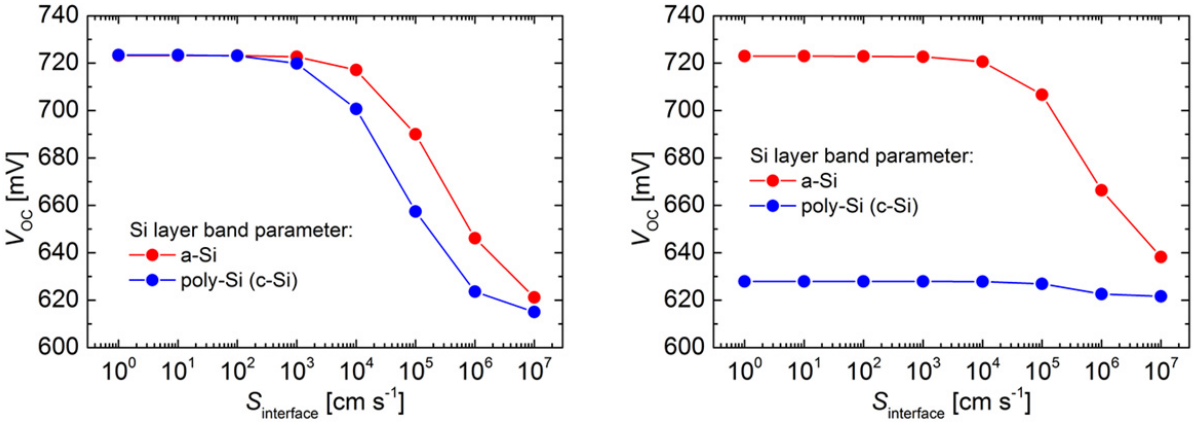

Fig. 5. Open circuit voltage V_{OC} plotted against the interface recombination velocity $S_{interface}$ for different band parameters for the doped Si layer. The results for a-Si (red) and poly-Si represented by the band parameters of c-Si (red) are plotted for simulation performed with tunnel oxide (left) and without tunnel oxide (right).

Fig. 5 shows that for the investigated parameters there are two possibilities of introducing a carrier selective contact, i.e. to avoid recombination at the Si layer / metal interface:

- By introducing a tunnel oxide below the Si layer (left)
- By using a high band gap material for the Si layer (right, red)

For these three structures the V_{OC} is on a very high level for surface recombination velocities below $S_{interface} = 10^3$ cm s^{-1} representing a good chemical passivation. The V_{OC} decreases for higher $S_{interface}$ as recombination at the c-Si / oxide (left) or c-Si / Si layer interface (right) becomes dominant.

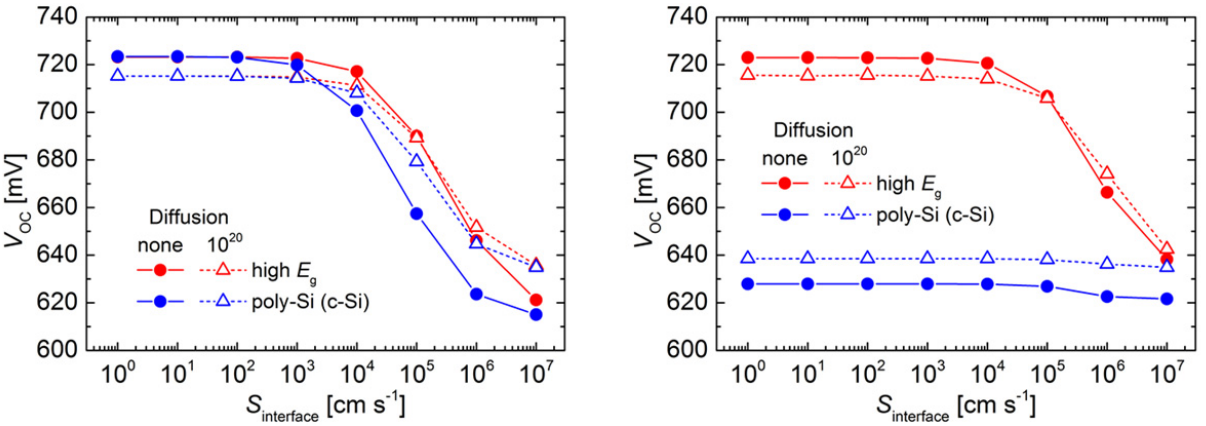

Fig. 6. V_{OC} plotted against $S_{interface}$ for different band parameters for the doped Si layer, similar to Fig. 5 but with an additional in-diffusion in the bulk material (open triangles). Again, the device is simulated with oxide (left) and without oxide (right).

Fig. 6 shows the influence of an additional (n^{++}) in-diffusion in the bulk material (dotted lines with open triangles) on the V_{OC} of the device. The latter may occur due to high temperature processes during cell fabrication. An

additional highly doped n^{++} region in the bulk material is not beneficial for the V_{OC} if the device features a good surface passivation (low $S_{interface}$ values). For high peak concentrations of the diffusion, the V_{OC} is even reduced due to Auger recombination in the diffusion region.

The reason for the low recombination and therefore the high V_{OC} (with tunnel oxide and for moderate surface recombination velocities of up to $S_{interface} = 10^3$ cm s^{-1}) even without diffusion is the induced band bending in the bulk material. This band bending originates from the high doping of the rear Si layer. The band structures, corresponding to the high band gap material and with tunnel oxide (compare Fig. 6, left), are shown in Fig. 7.

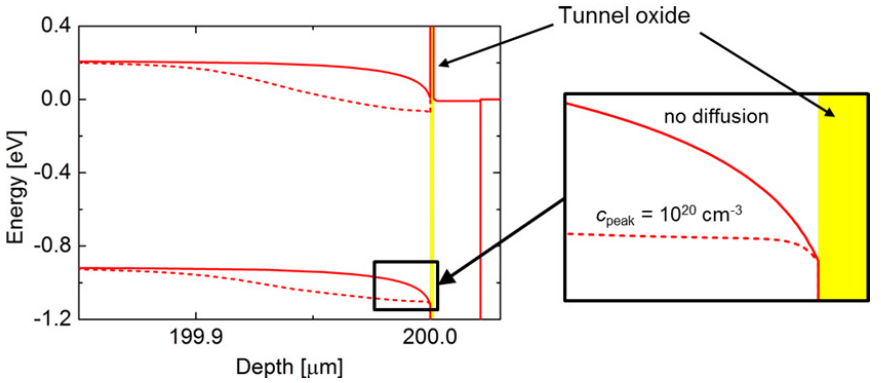

Fig. 7. The band structure of a carrier-selective contact featuring a tunnel oxide (yellow) and a highly doped high band gap material at the rear is plotted without (solid lines) and with an additional in-diffusion (dotted lines) in the bulk material (corresponding to Fig. 6, left).

The detailed view of the valence band in Fig. 7 (right, solid line) shows very well the shallow induced band bending. For cells where recombination at the interface is dominant or cells featuring a low band gap material and no tunnel oxide the additional diffusion, which is much deeper than the induced band bending, improves the cell performance due to a lower minority carrier concentration close to the the c-Si / oxide or c-Si / Si layer interface, respectively.

However, an in-diffusion in the bulk material also affects the majority carrier (electron) transport through the tunnel oxide. A higher electron concentration close to the oxide interface, originating from an additional in-diffusion, enhances the electron tunneling current through the tunnel oxide (compare Fig. 4). Therefore a moderate diffusion, without significant reduction of the V_{OC} due to Auger recombination, may improve the overall cell performance.

4. Conclusion and outlook

We discussed different experimental approaches for carrier-selective contacts featuring thin oxide interlayers based on different materials (poly-crystalline and amorphous) by means of numerical device simulation. A passivating and carrier-selective contact can be established in two different ways: (i) the use of a thin tunnel oxide or (ii) the application of a high band gap material. An additional in-diffusion in the bulk material, which may occur due to high temperature processes during cell fabrication is not beneficial for the recombination properties of a device featuring a good surface passivation. It reduces the V_{OC} due to Auger recombination in the diffusion region.

For the majority carrier transport and therefore the fill factor of the device such an in-diffusion can improve the device performance depending also on the applied doping of the Si layer, the tunnel oxide thickness and the assumed tunnelling mass. Further analysis on this topic including additional parameters, more detailed parameter variations and the discussion of the majority carrier transport properties by means of a fill factor analysis will be presented in a future publication.

Acknowledgements

Part of this work was funded by the German Federal Ministry for Economic Affairs and Energy under contract numbers 0325292 (“ForTeS”), 0325447 (“OHM”) and 0325634 (“INNOHET”).

References

[1] F. Feldmann, M. Bivour, C. Reichel, M. Hermle, and S. W. Glunz, "A passivated rear contact for high-efficiency n-type silicon solar cells enabling high V_{oc}S and FF>82%," in *Proceedings of the 28th EUPVSEC*, Paris, France, 2013, 988-92.

[2] J. B. Heng, F. Jianming, B. Kong, C. Yongkee, W. Wei, X. Zhigang, A. Reddy, K. Lam, C. Beitel, C. Liao, C. Erben, H. Zhiquan, and X. Zheng, ">23% High-Efficiency Tunnel Oxide Junction Bifacial Solar Cell With Electroplated Cu Gridlines," *Photovoltaics, IEEE Journal of*, 2015, 5, 82-86.

[3] U. Römer, R. Peibst, T. Ohrdes, B. Lim, J. Krügener, E. Bugiel, T. Wietler, and R. Brendel, "Recombination behavior and contact resistance of n+ and p+ poly-crystalline Si/mono-crystalline Si junctions," *Sol. Energy Matter. Sol. Cells*, 2014, 131, 85-91.

[4] F. Feldmann, M. Bivour, C. Reichel, H. Steinkemper, M. Hermle, and S. W. Glunz, "Tunnel oxide passivated contacts as an alternative to partial rear contacts," *Solar Energy Materials and Solar Cells*, 2014, 131, 46-50.

[5] R. Peibst, U. Römer, K. R. Hofmann, B. Lim, T. F. Wietler, Kru, J. gener, N. P. Harder, and R. Brendel, "A Simple Model Describing the Symmetric I-V Characteristics of p Polycrystalline Si/n Monocrystalline Si, and n Polycrystalline Si/p Monocrystalline Si Junctions," *IEEE Journal of Photovoltaics*, 2014, 4, 841-850.

[6] J. Shewchun, R. Singh, and M. A. Green, "Theory of metal-insulator-semiconductor solar cells," *Journal of Applied Physics*, 1977, 48, 765-70.

[7] Synopsys. (2013). *Synopsys TCAD, release H-2013.03*. Available: http://www.synopsys.com

[8] J. Greulich, N. Wöhrle, M. Glatthaar, and S. Rein, "Optical modeling of the rear surface roughness of passivated silicon solar cells," *Energy Procedia*, 3-5 Apr 2012, 27, 234-9.

[9] N. Wöhrle, J. Greulich, C. Schwab, M. Glatthaar, and S. Rein, "A predictive optical simulation model for the rear-surface roughness of passivated silicon solar cells," *IEEE Journal of Photovoltaics*, 2013, 3, 175-82.

[10] W. G. J. H. M. van Sark, L. Korte, and F. Roca, Eds., *Physics and Technology of Amorphous-Crystalline Heterostructure Silicon Solar Cells* (Engineering Materials. Springer 2012, 582 pages.

[11] P. P. Altermatt, "Models for numerical device simulations of crystalline silicon solar cells—a review," *Journal of Computational Electronics*, 2011, 10, 314-30.

[12] A. Richter, S. W. Glunz, F. Werner, J. Schmidt, and A. Cuevas, "Improved quantitative description of Auger recombination in crystalline silicon," *Physical Review B*, 2012, 86, 1-14.

[13] M. Ieong, P. M. Solomon, S. E. Laux, H. S. P. Wong, and D. Chidambarrao, "Comparison of raised and Schottky source/drain MOSFETs using a novel tunneling contact model," in *IEDM '98. Technical Digest., International*, 1998, 733-736.